Accepted Manuscript

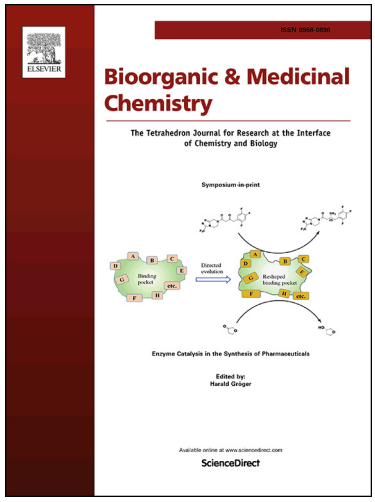

Antioxidant, anti-tyrosinase and anti-melanogenic effects of (*E*)-2,3-diphenylacrylic acid derivatives

Sultan Ullah, Yujin Park, Chaeun Park, Sanggwon Lee, Dongwan Kang, Jungho Yang, Jinia Akter, Pusoon Chun, Hyung Ryong Moon

PII: S0968-0896(19)30388-8
DOI: https://doi.org/10.1016/j.bmc.2019.04.020
Reference: BMC 14874

To appear in: *Bioorganic & Medicinal Chemistry*

Received Date: 7 March 2019
Revised Date: 12 April 2019
Accepted Date: 13 April 2019

Please cite this article as: Ullah, S., Park, Y., Park, C., Lee, S., Kang, D., Yang, J., Akter, J., Chun, P., Moon, H.R., Antioxidant, anti-tyrosinase and anti-melanogenic effects of (*E*)-2,3-diphenylacrylic acid derivatives, *Bioorganic & Medicinal Chemistry* (2019), doi: https://doi.org/10.1016/j.bmc.2019.04.020

Antioxidant, anti-tyrosinase and anti-melanogenic effects of (*E*)-2,3-diphenylacrylic acid derivatives

Sultan Ullah[a,§], Yujin Park[a,§], Chaeun Park[a], Sanggwon Lee[a], Dongwan Kang[a], Jungho Yang[a], Jinia Akter[a], Pusoon Chun[b], Hyung Ryong Moon[a,*]

[a]*Laboratory of Medicinal Chemistry, College of Pharmacy, Pusan National University, Busan 46241, South Korea*

[b]*College of Pharmacy and Inje Institute of Pharmaceutical Sciences and Research, Inje University, Gimhae, Gyeongnam 50834, South Korea*

[§]These authors (U. Sultan, and Y. Park) equally contributed to this work.

*****Author to whom correspondence should be addressed.

Hyung Ryong Moon, Laboratory of Medicinal Chemistry, College of Pharmacy, Pusan National University, Busan 46241, Republic of Korea. *E-mail address*: mhr108@pusan.ac.kr; Tel.: +82 51 510 2815; Fax: +82 51 513 6754.

Abstract

During our continued search for strong skin whitening agents over the past ten years, we have investigated the efficacies of many tyrosinase inhibitors containing a common (*E*)-β-phenyl-α,β-unsaturated carbonyl scaffold, which we found to be essential for the effective inhibition of mushroom and mammalian tyrosinases. In this study, we explored the tyrosinase inhibitory effects of 2,3-diphenylacrylic acid (2,3-DPA) derivatives, which also possess the (*E*)-β-phenyl-α,β-unsaturated carbonyl motif. We synthesized fourteen (*E*)-2,3-DPA derivatives **1a** – **1n** and one (*Z*)-2,3-DPA-derivative **1l'** using a Perkin reaction with phenylacetic acid and appropriate substituted benzaldehydes. In our mushroom tyrosinase assay, **1c** showed higher tyrosinase inhibitory activity (76.43±3.53%, IC_{50} = 20.04±1.91 μM) with than the other 2,3-DPA derivatives or kojic acid (21.56±2.93%, IC_{50} = 30.64±1.27 μM). Our mushroom tyrosinase inhibitory results were supported by our docking study, which showed compound **1c** (-7.2 kcal/mole) exhibited stronger binding affinity for mushroom tyrosinase than kojic acid (-5.7 kcal/mole). In B16F10 melanoma cells (a murine cell-line), **1c** showed no cytotoxic effect up to a concentration of 25 μM and exhibited greater tyrosinase inhibitory activity (68.83%) than kojic acid (49.39%). In these cells, arbutin (a well-known tyrosinase inhibitor used as the positive control) only inhibited tyrosinase by 42.67% even at a concentration of 400 μM. Furthermore, at 25 μM, **1c** reduced melanin contents in B16F10 melanoma cells by 24.3% more than kojic acid (62.77% vs. 38.52%). These results indicate **1c** is a promising candidate treatment for pigmentation-related diseases and potential skin whitening agents.

Key words: 2,3-diphenylacrylic acid, Perkin reaction, tyrosinase, inhibitor, B16F10 melanoma cells, skin whitening.

1. Introduction

A white skin appearance is viewed as an attractive feature by today's fashion industry. According to recent surveys, almost fifteen percent of the world's population purchase skin whitening products[1]. Numbers of users continue to increase, and the world market for skin whitening products has been predicted to reach $ 23 billion by 2020.[2] Many substances influence skin color, and melanin is the most important substance in skin that determines color. Melanin is a dark pigment produced by melanocytes in skin by a process called melanogenesis.[3,4] Melanocytes are derived from melanoblasts and reside in the basal skin layer surrounded by keratinocytes[5], and during melanogenesis, melanocytes accumulate melanin in melanosomes, and subsequently, it is transported to keratinocytes through dendrites.[6,7] Melanin protects skin against various noxious challenges like those posed by UV radiation, toxic chemicals, drugs, and environmental toxicants[2]. However, irregular melanin production causes various skin problems such as age spots, melasma, pigmented acne, lentigo, freckles, post-inflammatory melanoderma and scar-associated pigmentation.[8-11] In addition to melanogenesis disorders, melanin has also been associated with neurodegenerative diseases such as Parkinson's, Huntington's, and Alzheimer's diseases.[12-16]

Tyrosinase is the enzyme responsible for the conversion of tyrosine to dopaquinone, which is the rate-limiting step during melanogenesis.[6,7] Dopaquinone is used as the substrate for biosynthesis of pheomelanin and eumelanin.[1,17] Since tyrosinase plays an important role in the production of melanin, many attempts have been made to develop skin lighting agents based on its inhibition.

2,3-Diphenylacrylic acid (2,3-DPA) derivatives have various biological activities, which include antiviral[18] and anticancer activities[19]. In addition, the anti-diabetic and anti-angiogenesis activities of some 2,3-DPA derivatives have been attributed to inhibitions of protein tyrosine phosphatase enzyme and vascular endothelial growth factor, respectively.[20,21] Some 2,3-DPA derivatives have also been used in sun creams[22] and in dry powder inhaler compositions for the treatment of asthma, chronic obstructive pulmonary disease, and other respiratory diseases.[23] Over the past 10 years, we have reported many tyrosinase inhibitors developed based on considerations of the chemical structures of L-tyrosine and L-dopa, that is, the natural substrates of tyrosinase.[24-29] During these studies, we found that the (*E*)-β-phenyl-α,β-unsaturated carbonyl scaffold is essential for the effective inhibition of mushroom and mammalian tyrosinases. Therefore, as part of our ongoing efforts to identify new, potent skin whitening agents, we designed (*E*)-2,3-diphenylacrylic acid ((*E*)-2,3-DPA) derivatives containing the (*E*)-β-phenyl-α,β-unsaturated carbonyl scaffold and synthesized fourteen (*E*)-2,3-DPA derivatives and one (*Z*)-2,3-DPA derivative. Based on measured mushroom tyrosinase inhibitory activities, the most potent (*E*)-2,3-DPA analog was assayed for cytotoxicity and cellular tyrosinase inhibitory activity and for the inhibition of melanogenesis in B16F10 cells.

2. Results and Discussions

2.1. Chemistry

A schematic for the preparation of (*E*)-2,3-DPA derivatives is shown in Scheme 1. We considered these derivatives could be produced using the Perkin reaction because this reaction between benzaldehydes and phenylacetic acids is known to favour production of the (*E*)-stereoisomer.[30,31] Perkin reactions between hydroxy- or methoxy-substituted benzaldehydes and phenylacetic acid afforded *O*-acetylated (*E*)-2,3-DPA derivatives (**2a** – **2l**) and (*E*)-2,3-DPA derivatives (**1m** and **1n**), respectively. Interestingly, Perkin reaction between 3,5-dibromo-4-hydroxybenzaldehyde and

phenylacetic acid produced *O*-acetylated (*Z*)-2,3-DPA derivative **2l′** as well as *O*-acetylated (*E*)-2,3-DPA derivative **2l** in a 2:1 ratio (yields of 44% and 20%, respectively). To the best of our knowledge, this is the first report of the synthesis of a (*Z*)-2,3-DPA derivative as the major product of a Perkin reaction. Previously Hadfield et al. synthesized (*E*)-3-(4-hydroxy-3-methoxyphenyl)-2-(3,4,5-trimethoxyphenyl)acrylic acid and confirmed its stereochemistry by comparing extinction coefficients and using the NOESY technique.[30] Thus, we confirmed the stereochemistries of derivatives **2l** and **2l′** by comparing the chemical shifts of vinylic protons (7.66 ppm for **2l** and 6.89 ppm for **2l′**) with the chemical shift of the vinylic proton (7.58 ppm) of the compound synthesized by Hadfield and co-workers. Conversion of the *O*-acetylated 2,3-DPA derivatives (**2a** – **2l** and **2l′**) into the desired 2,3-DPA derivatives (**1a** – **1l**, and **1l′**) was achieved using 1N-NaOH. The vinylic protons of all (*E*)-2,3-DPA derivatives (**1a** – **1l**) appeared in range of 7.53 – 8.15 ppm, indicating an (*E*)-geometry, whereas the vinylic proton of **1l′** appeared at 6.70 ppm, which indicated **2l′** was a (*Z*)-2,3-DPA derivative. The vinylic protons of compounds **1c** and **1h**, which possess a 2-hydroxyl group produced peaks downfield (at 8.00 and 8.15 ppm, respectively) of those of other (*E*)-2,3-DPA derivatives (7.53 – 7.90 ppm). This phenomenon has been previously reported for benzylidene derivatives.[25,32,33]

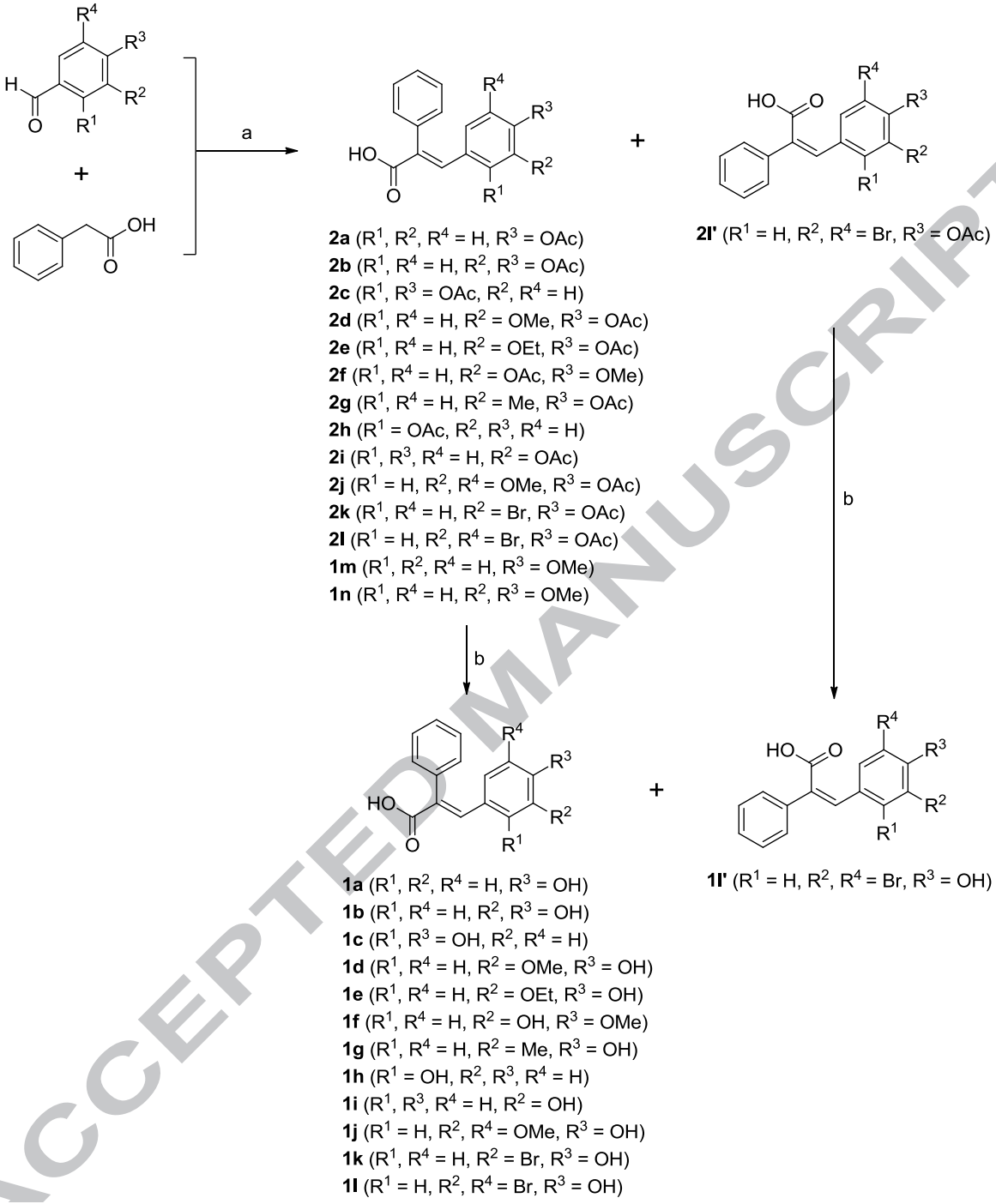

Scheme 1. Synthetic scheme for (*E*)-2,3-DPA derivatives 1a – 1n and (*Z*)-2,3-DPA derivative 1l′. Reagents and conditions: a) acetic anhydride, Et_3N, 90°C, 3 h, 20–73%; b) 1N-NaOH, 1,4-dioxane, room temperature, overnight, 88 – 99%.

*2.2. The mushroom tyrosinase inhibitory activities of (E)-2,3-DPA derivatives **1a – 1n***

The mushroom tyrosinase inhibitory activities of (*E*)-2,3-DPA derivatives **1a – 1n** and of the (*Z*)-2,3-DPA derivative **1l′** were evaluated at a concentration of 25 μM. Kojic acid (a well-known tyrosinase inhibitor) was used as a positive control at the same concentration. Tyrosinase inhibitory activities are summarized in Table 1. Four (*E*)-2,3-DPA derivatives (**1c**, **1d**, **1h**, and **1k**) potently inhibited mushroom tyrosinase. Although all 2,3-DPA derivatives contained the β-phenyl-α,β-unsaturated carbonyl motif, substitution patterns at the β-phenyl moiety greatly influenced the tyrosinase inhibition. Compound **1a** (12.78±3.86% inhibition) with a 4-hydroxyl group on the β-phenyl ring exhibited weaker tyrosinase inhibition than kojic acid (21.56±2.93% inhibition), but **1c** (76.43±3.53% inhibition, IC_{50} = 20.04±1.91 μM) with an additional hydroxyl group at the 2-position inhibited tyrosinase more than kojic acid (IC_{50} = 30.64±1.27 μM). On the other hand, compound **1b** (10.84±2.65% inhibition) with an additional hydroxyl group at the 3 position of **1a** did not exhibit any increase in inhibitory activity. Although the introduction of an additional hydroxyl group at the 3-position did not improve inhibitory activity, tyrosinase inhibition was enhanced by inserting a methoxyl group at the 3 position of **1a** (**1d**; 56.82±3.14% inhibition). Notably, insertion of a methyl group at the 3 position of **1a** did not increase inhibition (**1g**; 5.74±3.40% inhibition), and inserting an ethoxyl group at the 3 position (**1e**; 11.69±2.40% inhibition) did not increase inhibition. The low inhibition of **1e** was probably caused by an increase in steric hindrance. Interestingly, compound **1f** (10.55±1.59% inhibition), which had the same substituents as **1d**, but in the reverse positions had less inhibitory activity. Compound **1k** (43.86±2.63% inhibition) with an additional bromo group at the 3-position of **1a** increased inhibition as was observed for **1d**, whereas compounds **1l** and **1l′** with additional bromines at the 3 and 5 positions showed no increase in inhibition, regardless of their geometric dispositions. Like

1l and **1l′**, compound **1j** with additional methoxyl group at positions 3 and 5 of **1a** did not increase tyrosinase inhibitory activity. As was expected, compounds **1m** and **1n**, which did not possess a hydroxyl group, showed almost no inhibitory activity. On the other hand, compound **1h** (48.87±2.40% inhibition) with a 2-hydroxyl group on its β-phenyl showed a high level of tyrosinase inhibitory activity, whereas compound **1i** (6.78±2.86% inhibition) with a 3-hydroxy group on its β-phenyl showed only weak inhibitory activity. The above results indicate that the (*E*)-β-phenyl-α,β-unsaturated carbonyl motif is important for tyrosinase inhibition, and that substituents in appropriate positions on the β-phenyl ring also importantly influence the inhibition of tyrosinase.

Table 1. Tyrosinase inhibitory activities of (*E*)-2,3-DPA derivatives **1a** – **1n**, the (*Z*)-2,3-DPA derivative **1l′**, and kojic acid

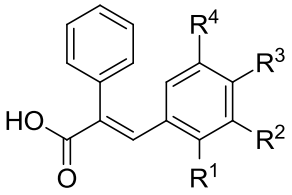

1a - 1n

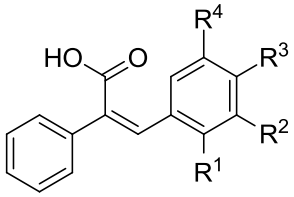

1l'

Compound	R^1	R^2	R^3	R^4	Tyrosinase inhibition (%)[α]
1a	H	H	OH	H	12.78±3.86
1b	H	OH	OH	H	10.84±2.65
1c	OH	H	OH	H	76.43±3.53
1d	H	OMe	OH	H	56.82±3.14
1e	H	OEt	OH	H	11.69±2.40
1f	H	OH	OMe	H	10.55±1.59
1g	H	Me	OH	H	5.74±3.40
1h	OH	H	H	H	48.87±2.40
1i	H	OH	H	H	6.78±2.86
1j	H	OMe	OH	OMe	5.63±2.88
1k	H	Br	OH	H	43.86±2.63
1l	H	Br	OH	Br	7.56±1.88
1l′	H	Br	OH	Br	13.20±2.80
1m	H	H	OMe	H	5.23±1.55
1n	H	OMe	OMe	H	3.40±2.67
Kojic acid					21.56±2.93

[α]Tyrosinase inhibitory activities were determined at a concentration of 25 μM. L-Tyrosine was used as a substrate. Results are presented as mean ± SEMs.

*2.3. Binding affinities and interactions between compound **1c** or kojic acid and tyrosinase.*

AutoDock Vina 1.1.2, a docking software package published by the Scripps Research Institute was used to determine the binding affinities and binding mode of compound **1c**, which exhibited the greatest inhibition of mushroom tyrosinase, was selected for the docking simulation. By using the energy minimization tool in Chem3D Pro ver. 12.0 from CambrigeSoft Corporation, we created a stable 3D structure of ligand **1c**; the 3D structure of tyrosinase was obtained from Protein Data Bank (ID: 2Y9X). As shown in Figure 1d, ligand **1c** showed greater binding affinity for tyrosinase (-7.2 kcal/mole) than kojic acid (-5.7 kcal/mole; the positive control). To investigate binding interactions between tyrosinase and ligand **1c**, we used LigandScout 4.2.1 software. As shown in Figure 1b, the positive control kojic acid exhibited π-π stacking interaction with His263, and formed two hydrogen bonds with His259 and His263. On the other hand, compound **1c** formed two hydrogen bonds with Asn260 and Met280, and exhibited hydrophobic interactions between its two phenyl groups and the two amino acids of tyrosinase at Phe264 and Val283 (Figures 1a and 1c). Accordingly, docking simulation results suggested the inhibitory effect of **1c** was due to strong binding with the active site of tyrosinase.

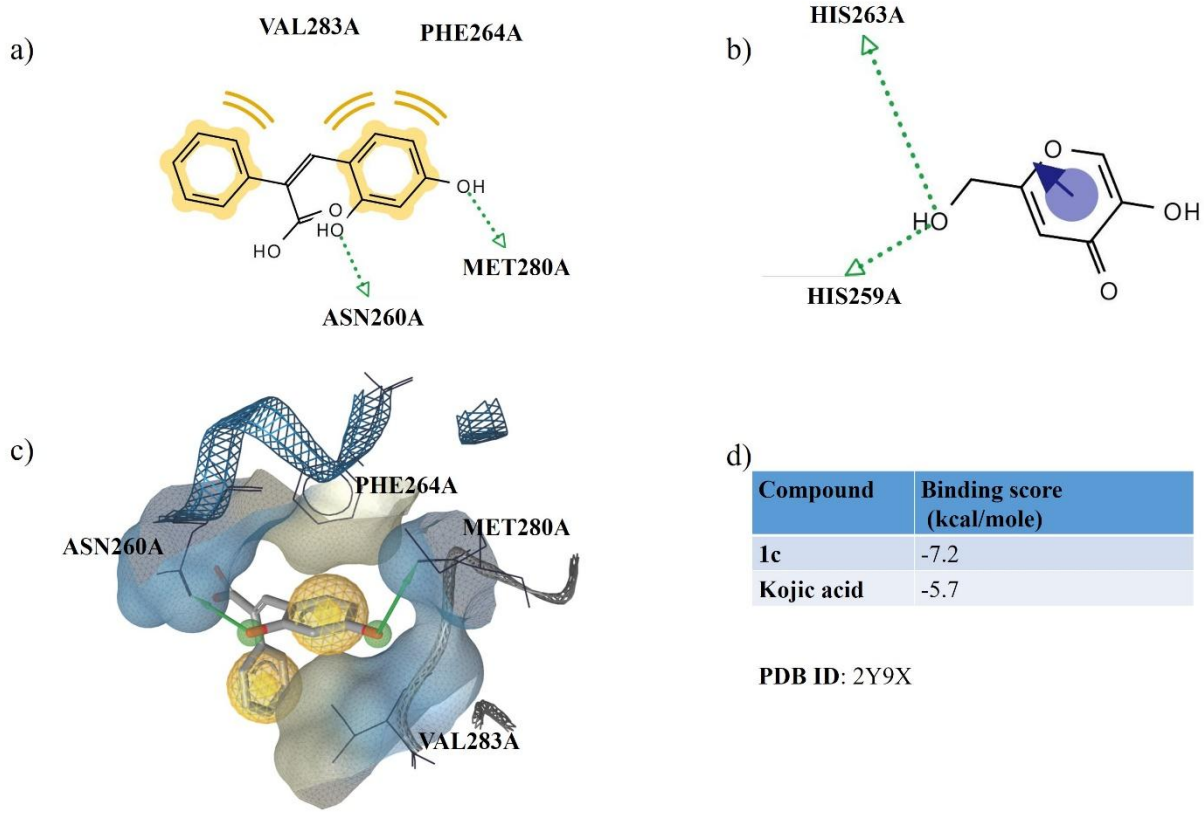

d)

Compound	Binding score (kcal/mole)
1c	-7.2
Kojic acid	-5.7

PDB ID: 2Y9X

Figure 1. Binding affinities and interactions between compound 1c or kojic acid and tyrosinase. (a, and b) Pharmacophore results of compound **1c** and kojic acid obtained using LigandScount 4.3.0 showing possible hydrogen-bonding (green arrows), π-π stacking (violet arrow), and hydrophobic interactions (yellow) between ligand **1c** or kojic acid and tyrosinase amino acids residues, (c) 3D pharmacophore model of ligand **1c** and tyrosinase, and (d) binding scores between ligand **1c** or kojic acid and tyrosinase.

*2.4. The cytotoxic effect of compound **1c** on B16F10 melanoma cells*

Of the 2,3-DPA derivatives synthesized, **1c** was chosen for cell viability analysis because it had the highest tyrosinase inhibitory activity in the mushroom tyrosinase assay. WST-8 assays were performed using B16F10 murine melanoma cells to check the safety of **1c**. B16F10 melanoma cells were treated with compound **1c** at concentrations of 0, 5, 10, or 25 μM in an incubator for 24 h. As shown in Figure 2, the safety profile of **1c** was satisfactory; only a negligible reduction in

cell numbers was observed at 25 μM. Thus, **1c** was deemed non-cytotoxic at concentrations below 25 μM.

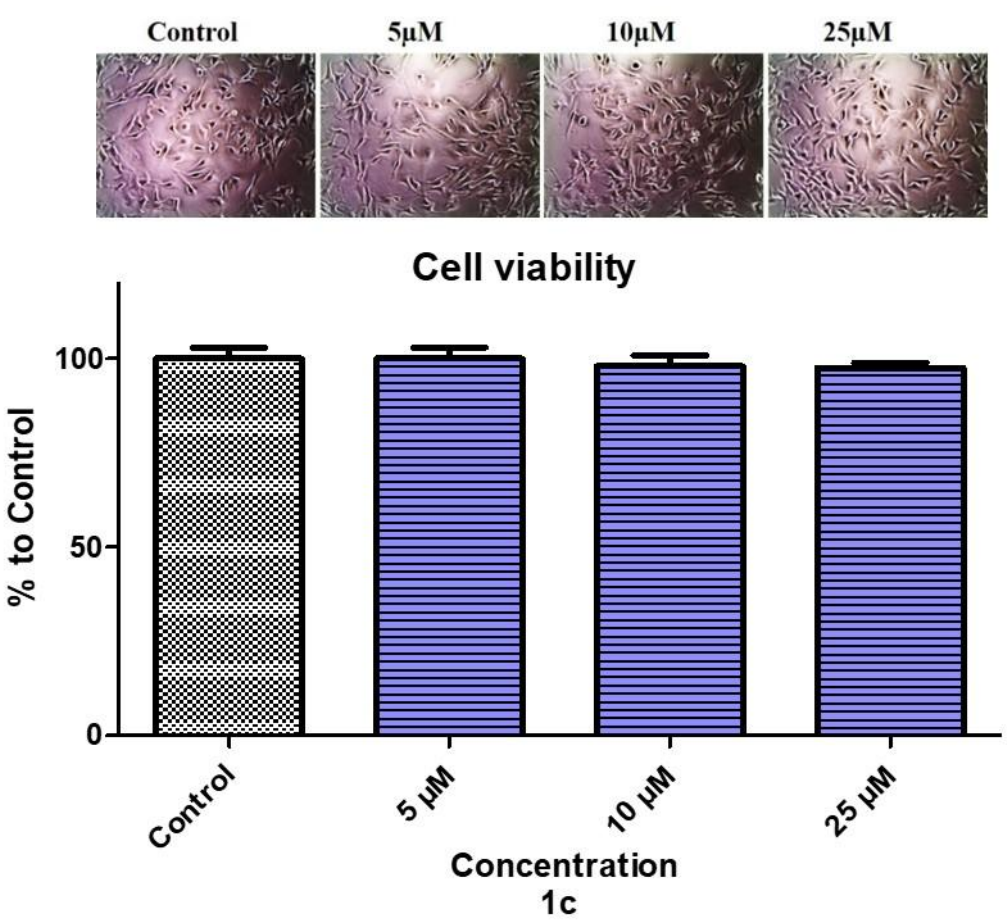

Figure 2. The cytotoxic effect of compound **1c** on B16F10 melanoma cells at concentrations of 5, 10, or 25 μM. Cytotoxic effects are expressed as percentages versus non-treated controls. Bars represent standard errors.

*2.5. The tyrosinase inhibitory effect of compound **1c in** B16F10 melanoma cells*

To evaluate the tyrosinase activity of **1c** with 2,4-dihydroxyphenyl further, B10F16 melanoma cells were stimulated with α-MSH and treated with **1c** at concentrations of 0, 5, 10, or 25 μM, kojic acid (25 μM) or arbutin (400 μM; the positive control). The cells were incubated in a 5% CO_2 environment for 24 h. Results are summarized in Figure 3.

As shown in Figure 3, compound **1c** more potently inhibited tyrosinase than kojic acid or arbutin. At 25 μM, **1c** and kojic acid inhibited tyrosinase activity by 68.83% and 49.39%, respectively, and arbutin at even 400 μM only inhibited its activity by 42.67%. Furthermore, compound **1c** inhibited tyrosinase activity in a concentration-dependent manner. These results indicate that the (*E*)-β-phenyl-α,β-unsaturated carbonyl motif potently inhibits both mushroom and mammalian tyrosinase. Notably, these results also showed that the presence of hydroxyl groups at the 2 and 4 positions of the β-phenyl ring importantly contribute to the inhibition of tyrosinase.

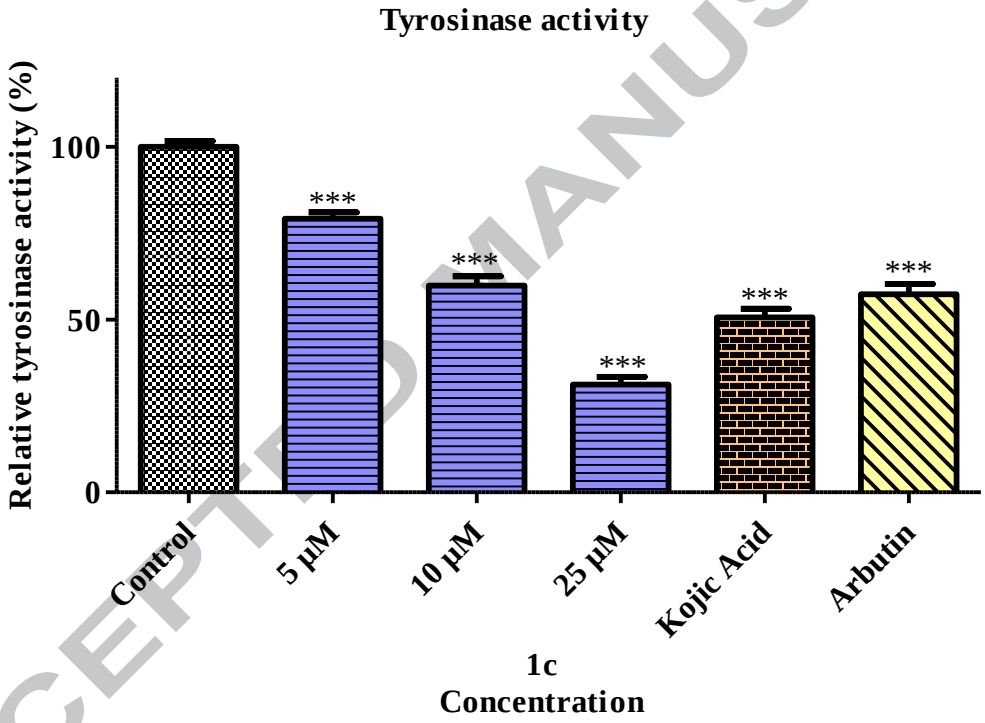

Figure 3. The tyrosinase inhibitory effects of compound **1c**, kojic acid (25 μM), and arbutin (400 μM) on α-MSH stimulated B16F10 melanoma cells. Asterisks *** indicate significant differences between columns ($p<0.001$). Standard errors are represented by bars.

2.6. The effect of compound 1c on the melanin contents of B16F10 melanoma cells

The anti-melanogenic effect of compound **1c** was investigated using the B16F10 melanoma cell

line. Initially, cells were activated with α-MSH and treated with compound **1c** (0, 5, 10, or 25 μM) or kojic acid (25 μM) for 24 h. Inhibitory effects on melanin production were quantified by measuring optical densities.

Treatment with compound **1c** at 25 μM significantly and more strongly reduced melanin levels than kojic acid at the same concentration (by 62.77% and 38.52%, respectively), which suggested **1c** had a greater inhibitory effect on tyrosinase (Figure 3). Furthermore, a comparison of Figures 3 and 4 revealed similar patterns of tyrosinase activity and melanin level inhibitions, which also indicated the antimelanogenic effect of **1c** was mainly due to tyrosinase inhibition.

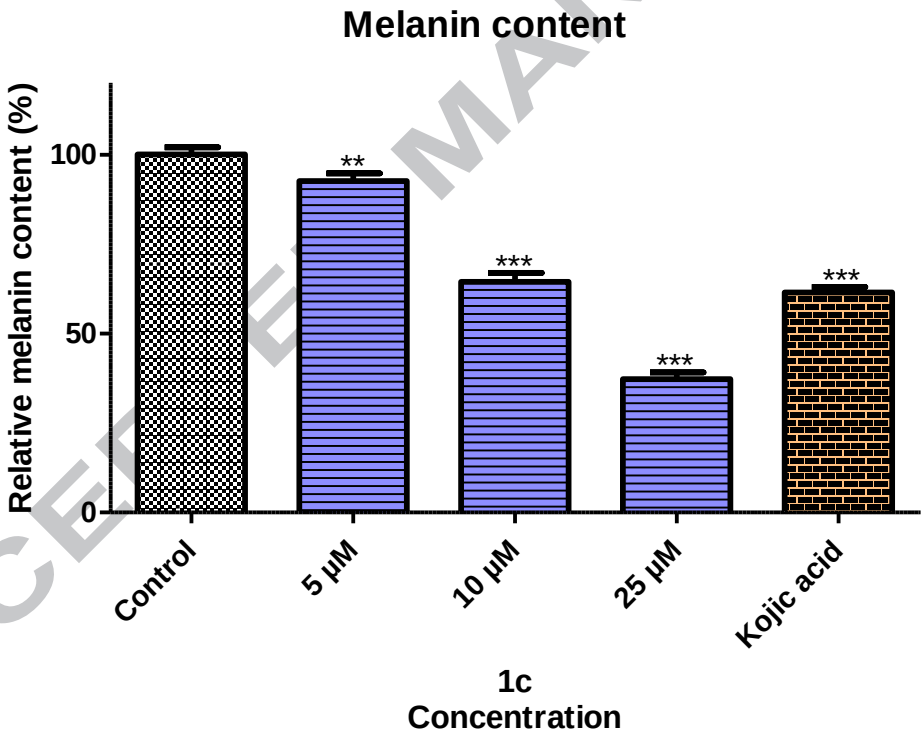

Figure 4. The effect of compound **1c** on the melanin contents of B16F10 melanoma cells stimulated by α-MSH. B16F10 cells were treated with compound **1c** (5, 10, or 25 μM) or kojic acid (25 μM). Asterisks indicate significant differences between columns: **, $p<0.01$; and ***, $p<0.001$. Standard errors are represented as bars.

*2.7. DPPH radical scavenging activities of (E)-2,3-DPA derivatives **1a** – **1n**, the (Z)-2,3-DPA derivative **1l'**, and of L-ascorbic acid*

DPPH radical scavenging assays were performed to assess the radical scavenging effects of the fifteen 2,3-DPA derivatives (**1a** – **1n** and **1l**′). 2,3-DPA derivatives and L-ascorbic acid were added at a concentration 1 mM to a solution of 0.2mM DPPH in methanol, and 30 min later, radical scavenging was assessed by measuring percentage absorbances. Results are summarized in Table 2.

According to our previously reported structure-activity data[26,27], compounds with a 3,4-dihydroxyl or 4-hydroxy-3-methoxyl substituent on the β-phenyl ring usually exhibit considerable DPPH radical scavenging activity. The results obtained for compounds **1b** (83.70±0.10 inhibition), which has a 3,4-dihydroxyl substituent, **1d** (81.56±0.23 inhibition), which has a 4-hydroxy-3-methoxyl substituent, and L-ascorbic acid (84.64±0.32 inhibition; positive control) were similar. Compounds **1g** (78.07±0.18 inhibition) and **1j** (85.03±1.07 inhibition), which possess a 4-hydroxy-3-methyl and a 4-hydroxy-3,5-dimethoxyl substituent, respectively, had almost the same potency as L-ascorbic acid. However, the other 2,3-DPA derivatives exhibited only weak to moderate radical scavenging activity. Furthermore, it has been well established that reactive oxygen species increase tyrosinase expression, and thus, positively affect melanin production, which suggests the antioxidant activities of 2,3-DPA derivatives may partially contribute to the reduction of melanin levels.

Table 1. DPPH radical scavenging activities of (*E*)-2,3-DPA derivatives **1a** – **1n**, the (*Z*)-2,3-DPA derivative **1l′**, and of *L-ascorbic acid*.

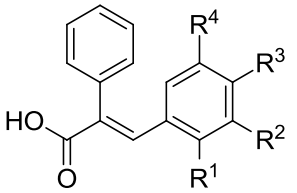

1a - 1n

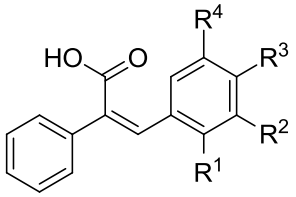

1l'

Compound	DPPH Radical scavenging activity (%)	Compound	DPPH Radical scavenging activity (%)
1a	6.04±0.40	**1i**	12.43±2.22
1b	83.70±0.10	**1j**	85.03±1.07
1c	52.11±0.59	**1k**	19.42±0.36
1d	81.56±0.23	**1l**	23.88±0.45
1e	43.58±1.50	**1l′**	11.56±0.34
1f	24.04±0.19	**1m**	5.68±1.22
1g	78.07±0.18	**1n**	10.16±1.15
1h	4.43±0.33	L-ascorbic acid	84.64±0.32

The radical scavenging effects of the fifteen 2,3-DPA derivatives (**1a – 1n** and **1l′**) and of L-ascorbic acid were measured at a concentration of 1 mM. Three independent experiments were performed and results are expressed as means ± standard deviations.

3. Conclusion

Fourteen (*E*)-2,3-DPA derivatives **1a** – **1n** and one (*Z*)-2,3-DPA derivative **1l′** containing the (*E*)-β-phenyl-α,β-unsaturated carbonyl motif were synthesized using phenylacetic acid and substituted benzaldehydes. This is the first report of the production of a (*Z*)-2,3-DPA derivative **1l′** as the major product using the Perkin reaction. The tyrosinase inhibitory effects of these fifteen compounds were evaluated using mushroom tyrosinase. The (*E*)-2,3-DPA derivative **1c** most inhibited tyrosinase activity (76.43±3.53% inhibition at 25 μM), and this inhibition also exceeded that of kojic acid (21.56±2.93% inhibition at 25 μM). Our results show tyrosinase inhibition is dependent on substituent type(s) and location(s) on the β-phenyl ring of the (*E*)-β-phenyl-α,β-unsaturated carbonyl motif. Furthermore, our experimental mushroom tyrosinase inhibitory results were supported by the docking study, according to which compound **1c** (-7.2 kcal/mole) exhibited stronger binding to tyrosinase than kojic acid (-5.7 kcal/mole). B16F10 melanoma cells were used to investigate the cytotoxicity of derivative **1c**, and its effects on cellular tyrosinase activity and melanin contents. We found **1c** was not cytotoxic to B16F10 melanoma at concentrations up to 25 μM, and at a concentration of 25 μM inhibited tyrosinase activity significantly more than kojic acid (25 μM) and arbutin (400 μM). Furthermore, **1c** at the same concentration reduced melanin contents 24.3% more than kojic acid. These results indicate **1c** is a promising candidate for treating hyperpigmentation-related diseases.

4. Experimental Section

4.1. Chemistry

All reactions were monitored by thin layer chromatography (TLC), which was performed using Merk 60 F_{254} glass silica gel plates. All intermediates and final products were purified by extraction, recrystallization, and MP silica 40–63 (60 Å) column chromatography. Structures were elucidated using a Varian Unity INOVA ^{1}H NMR and a ^{13}C NMR spectrophotometer (Agilent Technologies, Santa Clara, CA, USA) using DMSO-d_6, $CDCl_3$ and CD_3OD as solvents. All chemical shifts were measured in ppm (parts per million) against residual solvents or deuterated peaks (for DMSO-d_6 δ_H 2.50 and δ_C 39.7, and for $CDCl_3$ δ_H 7.24 and δ_C 77.0). Coupling constants are presented in Hertz. The following abbreviations were used in the analysis of NMR data: s (singlet), brs (broad singlet), d (doublet), dd (doublet of doublets), brd (broad doublet), t (triplet), q (quartet) and m (multiplet). Mass spectrometers were used to determine the masses of the synthesized 2,3-DPA derivatives. Low-resolution mass spectra were recorded on an Expression CMS from Advion Ithaca, NY, USA, and high-resolution mass spectra were recorded using an Agilent Accurate-Mass Q-TOF liquid chromatography/mass spectrometer from Agilent, Santa Clara, CA, USA.

4.1.1. **General procedure for the syntheses of 2a – 2n, and 2l′, 1m and 1n**

Substituted benzaldehydes (70 mg) and phenylacetic acid (1.0 equiv.) were added to a 25 mL round bottom flask and then 1.5 mL of acetic anhydride and 0.7 mL of triethylamine were added sequentially. This reaction mixture was then stirred at 90^0C for 3 h. On completion of the reaction, conc. HCl was added at 0^0C and the pH was adjusted to 2. The reaction mixture was then partitioned between ethyl acetate and water, and the organic layer was dried over anhydrous $MgSO_4$, filtered, and evaporated under reduced pressure. The residue was then purified either by

recrystallization from ethanol or column chromatography using hexane/ethyl acetate gradient elution at 2–5:1 to give 2,3-DPA derivatives **2a** – **2l**, **2l′**, **1m**, and **1n** as solids in yields of 20 – 73%.

4.1.1.1. (*E*)-3-(4-Acetoxyphenyl)-2-phenylacrylic acid (2a). Yellowish white solid, 44% yield. ^{1}H NMR (400 MHz, $CDCl_3$) δ 7.88 (s, 1 H, vinylic H), 7.37 – 7.34 (m, 3 H, 3-H, 4-H, 5-H), 7.22 (d, 2 H, J = 7.6 Hz, 2-H, 6-H), 7.04 (d, 2 H, J = 8.4 Hz, 2′-H, 6′-H), 6.87 (d, 2 H, J = 8.4 Hz, 3′-H, 5′-H), 2.23 (s, 3 H, Ac); ^{13}C NMR (100 MHz, $CDCl_3$) δ 172.7, 169.3, 151.5, 141.4, 135.3, 132.2, 132.1, 129.9, 129.0, 128.9, 128.3, 121.7, 21.3.

4.1.1.2. (*E*)-3-(3,4-Diacetoxyphenyl)-2-phenylacrylic acid (2b). Brown solid, 67% yield. ^{1}H NMR (500 MHz, $CDCl_3$) δ 7.86 (s, 1 H, vinylic H), 7.41 – 7.37 (m, 3 H, 3-H, 4-H, 5-H), 7.24 (d, 2 H, J = 7.5 Hz, 2-H, 6-H), 6.99 (d, 1 H, J = 9.0 Hz, 6′-H), 6.93 (d, 1 H, J = 9.0 Hz, 5′-H), 6.87 (s, 1 H, 2′-H), 2.24 (s, 3 H, Ac), 2.21 (s, 3 H, Ac); ^{13}C NMR (100 MHz, $CDCl_3$) δ 172.7, 168.1, 143.0, 141.9, 140.5, 134.8, 133.2, 132.7, 129.8, 129.2, 129.1, 128.5, 126.0, 123.4, 20.8, 20.7.

4.1.1.3. (*E*)-3-(2,4-Diacetoxyphenyl)-2-phenylacrylic acid (2c). Brown solid, 73% yield. ^{1}H NMR (500 MHz, $CDCl_3$) δ 7.90 (s, 1 H, vinylic H), 7.35 – 7.32 (m, 3 H, 3-H, 4-H, 5-H), 7.24 (d, 2 H, J = 7.5 Hz, 2-H, 6-H), 6.93 (d, 1 H, J = 1.5 Hz, 3′-H), 6.76 (d, 1 H, J = 8.5 Hz, 5′-H), 6.66 (d, 1 H, J = 8.5, 1.5 Hz, 6′-H), 2.37 (s, 3 H, Ac), 2.24 (s, 3 H, Ac); ^{13}C NMR (100 MHz, $CDCl_3$) δ 172.6, 169.0, 168.8, 151.6, 150.5, 135.2, 134.6, 133.7, 131.2, 130.1, 128.8, 128.4, 125.3, 118.9, 116.2, 21.3, 21.1.

4.1.1.4. (*E*)-3-(4-Acetoxy-3-methoxyphenyl)-2-phenylacrylic acid (2d). Yellowish white solid, 66% yield. ^{1}H NMR (400 MHz, $CDCl_3$) δ 7.86 (s, 1 H, vinylic H), 7.39 – 7.33 (m, 3 H, 3-H, 4-H, 5-H), 7.24 (d, 2 H, J = 7.6 Hz, 2-H, 6-H), 6.88 (d, 1 H, J = 8.4 Hz, 5′-H), 6.80 (d, 1 H, J = 8.4 Hz,

6′-H), 6.50 (s, 1 H, 2′-H), 3.32 (s, 3 H, OCH_3), 2.24 (s, 3 H, Ac); ^{13}C NMR (100 MHz, $CDCl_3$) δ 172.8, 168.9, 150.7, 141.8, 140.9, 135.6, 133.1, 131.6, 130.0, 129.1, 128.3, 125.1, 122.8, 113.9, 55.4, 20.8.

4.1.1.5. (*E*)-3-(3-Acetoxy-4-ethoxyphenyl)-2-phenylacrylic acid (2e). White solid, 54% yield. ^1H NMR (400 MHz, $CDCl_3$) δ 7.85 (s, 1 H, vinylic H), 7.38 (t, 2 H, J = 7.6 Hz, 3-H, 5-H), 7.33 (t, 1 H, J = 7.6 Hz, 4-H), 7.24 (d, 2 H, J = 7.6 Hz, 2-H, 6-H), 6.86 (d, 1 H, J = 8.4 Hz, 5′-H), 6.77 (d, 1 H, J = 8.4, 1.6 Hz, 6′-H), 6.49 (d, 1 H, J = 1.6 Hz, 2′-H), 3.50 (q, 2 H, J = 7.2 Hz, CH_2CH_3), 2.23 (s, 3 H, Ac), 1.14 (t, 3 H, J = 7.2 Hz, CH_2CH_3); ^{13}C NMR (100 MHz, $CDCl_3$) δ 172.6, 168.9, 150.0, 141.8, 141.2, 135.6, 133.0, 131.5, 130.0, 129.1, 128.2, 124.9, 122.7, 114.9, 63.9, 20.7, 14.7.

4.1.1.6. (*E*)-3-(3-Acetoxy-4-methoxyphenyl)-2-phenylacrylic acid (2f). Yellowish white solid, 68% yield. ^1H NMR (500 MHz, $CDCl_3$) δ 7.84 (s, 1 H, vinylic H), 7.41 – 7.36 (m, 3 H, 3-H, 4-H, 5-H), 7.24 (d, 2 H, J = 7.5 Hz, 2-H, 6-H), 6.93 (d, 1 H, J = 8.5 Hz, 6′-H), 6.74 (d, 1 H, J = 8.5 Hz, 5′-H), 6.71 (s, 1 H, 2′-H), 3.78 (s, 3 H, OCH_3), 2.23 (s, 3 H, Ac); ^{13}C NMR (100 MHz, $CDCl_3$) δ 172.9, 168.9, 152.4, 141.4, 139.4, 135.5, 130.4, 130.1, 129.9, 129.1, 128.2, 127.4, 125.6, 112.0, 56.1, 20.8.

4.1.1.7. (*E*)-3-(4-Acetoxy-3-methylphenyl)-2-phenylacrylic acid (2g). Yellowish White solid, 47% yield. ^1H NMR (400 MHz, $CDCl_3$) δ 7.85 (s, 1 H, vinylic H), 7.36 – 7.33 (m, 3 H, 3-H, 4-H, 5-H), 7.21 (d, 2 H, J = 7.6 Hz, 2-H, 6-H), 6.92 (d, 1 H, J = 2.0 Hz, 2′-H), 6.84 (dd, 1 H, J = 8.4, 2.0 Hz, 6′-H), 6.77 (d, 1 H, J = 8.4 Hz, 5′-H), 2.25 (s, 3 H, CH_3), 1.98 (s, 3 H, Ac); ^{13}C NMR (100 MHz, $CDCl_3$) δ 172.9, 169.1, 150.3, 141.6, 135.4, 133.3, 132.3, 131.7, 130.3, 129.9, 129.7, 129.0, 128.3, 122.1, 21.0, 16.3.

4.1.1.8. (*E*)-3-(2-Acetoxyphenyl)-2-phenylacrylic acid (2h). White solid, 51% yield. ^1H NMR

(400 MHz, $CDCl_3$) δ 7.91 (s, 1 H, vinylic H), 7.30 – 7.27 (m, 3 H, 3-H, 4-H, 5-H), 7.23 – 7.19 (m, 3 H, 2-H, 6-H, 5′-H), 7.02 (d, 1 H, J = 8.0 Hz, 6′-H), 6.86 (t, 1 H, J = 8.0 Hz, 4′-H), 6.74 (d, 1 H, J = 8.0 Hz, 3′-H), 2.35 (s, 3 H, Ac); ^{13}C NMR (100 MHz, $CDCl_3$) δ 172.3, 169.5, 150.0, 136.0, 134.8, 134.0, 130.8, 130.4, 130.2, 128.6, 128.3, 128.0, 125.7, 122.6, 21.1.

4.1.1.9. (*E*)-3-(3-Acetoxyphenyl)-2-phenylacrylic acid (2i). Off-white solid, 74% yield. ^{1}H NMR (500 MHz, $CDCl_3$) δ 7.89 (s, 1 H, vinylic H), 7.39 – 7.31 (m, 3 H, 3-H, 4-H, 5-H), 7.24 (d, 2 H, J = 7.5 Hz, 2-H, 6-H), 7.16 (t, 1 H, J = 7.5 Hz, 5′-H), 6.95 (d, 1 H, J = 7.5 Hz, 4′- or 6′-H), 6.90 (d, 1 H, J = 7.5 Hz, 4′- or 6′-H), 6.77 (s, 1 H, 2′-H), 2.21 (s, 3 H, Ac); ^{13}C NMR (100 MHz, $CDCl_3$) δ 172.4, 169.4, 150.6, 141.1, 136.1, 135.2, 133.1, 129.9, 129.4, 129.0, 128.3, 124.0, 122.8, 21.2.

4.1.1.10. (*E*)-3-(4-Acetoxy-3,5-dimethoxyphenyl)-2-phenylacrylic acid (2j). Yellowish grey solid, 47% yield. ^{1}H NMR (500 MHz, DMSO-d_6) δ 12.66 (brs, 1 H, COOH), 7.73 (s, 1 H, vinylic H), 7.42 (t, 2 H, J = 7.5 Hz, 3-H, 5-H), 7.35 (t, 1 H, J = 7.5 Hz, 4-H), 7.20 (d, 2 H, J = 7.5 Hz, 2-H, 6-H), 6.44 (s, 2 H, 2′-H, 6′-H), 3.41 (s, 6 H, 2 x OCH_3), 2.17 (s, 3 H, Ac); ^{13}C NMR (100 MHz, DMSO-d_6) δ 168.8, 168.5, 151.8, 139.3, 137.2, 134.1, 133.0, 130.1, 129.3, 129.1, 128.2, 108.0. 56.1, 20.7.

4.1.1.11. (*E*)-3-(4-Acetoxy-3-bromophenyl)-2-phenylacrylic acid (2k). Yellowish white solid, 36% yield. ^{1}H NMR (500 MHz, $CDCl_3$) δ 7.83 (s, 1 H, vinylic H), 7.42 – 7.37 (m, 3 H, 3-H, 4-H, 5-H), 7.30 (s, 1 H, 2′-H), 7.22 (d, 2 H, J = 7.5 Hz, 2-H, 6-H), 6.98 (d, 1 H, J = 8.0 Hz, 6′-H), 6.91 (d, 1 H, J = 8.0 Hz, 5′-H), 2.31 (s, 3 H, Ac); ^{13}C NMR (100 MHz, $CDCl_3$) δ 172.4, 168.5, 148.9, 139.7, 135.7, 134.7, 134.0, 133.3, 131.1, 129.7, 129.1, 128.6, 123.6, 116.3, 21.0.

4.1.1.12. (*E*)-3-(4-Acetoxy-3,5-dibromophenyl)-2-phenylacrylic acid (2l). Yellow solid, 20% yield. ^{1}H NMR (500 MHz, $CDCl_3$) δ 7.66 (s, 1 H, vinylic H), 7.41 – 7.37 (m, 3 H, 3-H, 4-H, 5-H),

7.18 (brd, 2 H, *J* = 7.5 Hz, 2-H, 6-H), 7.16 (s, 2 H, 2′-H, 6′-H), 2.32 (s, 3 H, CH_3); ^{13}C NMR (100 MHz, $CDCl_3$ + 1 drop of CD_3OD) *δ* 169.1, 167.3, 146.3, 136.6, 135.6, 135.4, 134.9, 134.2, 129.5, 129.0, 128.5, 115.3, 20.5.

4.1.1.13. (*Z*)-3-(4-Acetoxy-3,5-dibromophenyl)-2-phenylacrylic acid (2l′). Brown solid, 44% yield. ^1H NMR (500 MHz, $CDCl_3$) *δ* 7.65 (s, 2 H, 2′-H, 6′-H), 7.48 (d, 2 H, *J* = 7.0 Hz, 2-H, 6-H), 7.40 – 7.36 (m, 3 H, 3-H, 4-H, 5-H), 6.87 (s, 1 H, vinylic H), 2.39 (s, 3 H, CH_3); ^{13}C NMR (100 MHz, $CDCl_3$) *δ* 171.4, 167.2, 146.1, 137.2, 136.3, 132.3, 129.1, 129.0, 127.0, 119.6, 117.9, 115.3, 20.6.

4.1.1.14. (*E*)-3-(4-Methoxyphenyl)-2-phenylacrylic acid (1m). Brownish yellow solid, 21% yield. ^1H NMR (500 MHz, $CDCl_3$) *δ* 7.90 (s, 1 H, vinylic H), 7.41 (t, 2 H, *J* = 7.5 Hz, 3-H, 5-H), 7.37 (t, 1 H, *J* = 7.5 Hz, 4-H), 7.25 (d, 2 H, *J* = 7.5 Hz, 2-H, 6-H), 7.01 (d, 2 H, *J* = 9.0 Hz, 2′-H, 6′-H), 6.69 (d, 2 H, *J* = 9.0 Hz, 3′-H, 5′-H), 3.76 (s, 3 H, OCH_3); ^{13}C NMR (100 MHz, CDC_{l3}) *δ* 173.1, 160.8, 142.3, 136.0, 132.9, 130.0, 129.2, 129.0, 128.1, 127.1, 114.0, 55.4; LRMS (ESI-) *m/z* 253 $(M-H)^-$.

4.1.1.15. (*E*)-3-(3,4-Dimethoxyphenyl)-2-phenylacrylic acid (1n). Yellowish grey, 31% yield. ^1H NMR (400 MHz, $CDCl_3$ + 1 drop of CD_3OD) *δ* 7.76 (s, 1 H, vinylic H), 7.35 (d, 2 H, *J* = 7.6 Hz, 3-H, 5-H), 7.27 (t, 1 H, *J* = 7.6 Hz, 4-H), 7.21 (d, 2 H, *J* = 7.6 Hz, 2-H, 6-H), 6.78 (dd, 1 H, *J* = 8.4, 2.0 Hz, 6′-H), 6.66 (d, 1 H, *J* = 8.4 Hz, 5′-H), 6.33 (d, 1 H, *J* = 2.0 Hz, 2′-H), 3.77 (s, 3 H, CH_3), 3.30 (s, 3 H, CH_3); ^{13}C NMR (100 MHz, CDC_{l3} + 1 drop of CD_3OD) *δ* 170.6, 150.2, 148.3, 141.2, 136.8, 130.1, 129.0, 127.9, 127.5, 125.9, 112.4, 110.6, 55.9, 55.2; LRMS (ESI-) *m/z* 283 $(M-H)^-$.

4.1.2. General procedure for the syntheses of 2,3-DPA derivatives 1a – 1l and 1l′

Compounds **2a – 2l**, and **2l′** (22.1 mg to 112.1 mg) were added to a 25 mL round bottom flask and then 1,4-dioxane (1 – 3 mL) and aqueous 1N-NaOH (4.0 equiv.) were sequentially added. The reaction was allowed to proceed at room temperature overnight with stirring. After completion of the reaction, aqueous 2N-HCl was added to the flask to adjust the pH to 2. The reaction mixture was then stirred at room temperature for 30 min and solid material was filtered. The filter cake so obtained was then washed with a large amount of water and dried to give 2,3-DPA derivatives **1a – 1l** and **2l′** in yields of 88 – 99%.

4.1.2.1. (*E*)-3-(4-Hydroxyphenyl)-2-phenylacrylic acid (1a). Yellowish white solid, 95% yield. ^{1}H NMR (500 MHz, $CDCl_3$ + 1 drop of CD_3OD) δ 7.76 (s, 1 H, vinylic H), 7.33 (t, 2 H, J = 7.5 Hz, 3-H, 5-H), 7.29 (t, 1 H, J = 7.5 Hz, 4-H), 7.18 (d, 2 H, J = 7.5 Hz, 2-H, 6-H), 6.85 (d, 2 H, J = 8.5 Hz, 2′-H, 6′-H), 6.54 (d, 2 H, J = 8.5 Hz, 3′-H, 5′-H); ^{13}C NMR (100 MHz, $CDCl_3$ + 1 drop of CD_3OD) δ 170.8, 158.2, 141.4, 136.7, 132.9, 129.9, 129.3, 128.9, 127.8, 126.4, 115.4; LRMS (ESI-) *m/z* 239 $(M-H)^-$.

4.1.2.2. (*E*)-3-(3,4-Dihydroxyphenyl)-2-phenylacrylic acid (1b). Brownish grey solid, 96% yield. ^{1}H NMR (400 MHz, DMSO-d_6) δ 12.34 (brs, 1 H, COOH), 9.43 (s, 1 H, OH), 8.78 (s, 1 H, OH), 7.53 (s, 1 H, vinylic H), 7.36 – 7.27 (m, 3 H, 3-H, 4-H, 5-H), 7.09 (d, 2 H, J = 7.6 Hz, 2-H, 6-H), 6.48 (d, 1 H, J = 8.0 Hz, 5′- or 6′-H), 6.38 (s, 1 H, 2′-H), 6.34 (d, 1 H, J = 8.0 Hz, 5′- or 6′-H); ^{13}C NMR (100 MHz, DMSO-d_6) δ 169.4, 147.7, 145.4, 140.3, 137.6, 130.2, 130.1, 129.1, 128.0, 126.3, 123.8, 118.4, 115.8; LRMS (ESI-) *m/z* 255 $(M-H)^-$, 211 $(M-H-CO_2)^-$.

4.1.2.3. (*E*)-3-(2,4-Dihydroxyphenyl)-2-phenylacrylic acid (1c). Yellowish brown solid, 98% yield. ^{1}H NMR (500 MHz, DMSO-d_6) δ 12.19 (brs, 1 H, COOH), 9.91 (s, 1 H, OH), 9.62 (s, 1 H, OH), 8.00 (s, 1 H, vinylic H), 7.34 (t, 2 H, J = 7.5 Hz, 3-H, 5-H), 7.28 (t, 1 H, J = 7.5 Hz, 4-H),

7.12 (d, 2 H, *J* = 7.5 Hz, 2-H, 6-H), 6.29 (s, 1 H, 3′-H), 6.26 (d, 1 H, *J* = 8.5 Hz, 6′-H), 5.80 (d, 1 H, *J* = 8.5 Hz, 5′-H); ^{13}C NMR (100 MHz, DMSO-d_6) δ 169.6, 160.5, 159.2, 138.2, 134.8, 131.1, 130.4, 129.0, 128.2, 127.7, 113.3, 107.4, 102.8; LRMS *m/z* 211 $(M\text{-}H\text{-}CO_2)^-$; HRMS (ESI+) m/z $C_{15}H_{13}O_4$ $(M+H)^+$ calcd 257.0808, obsd 257.0801, m/z $C_{15}H_{12}NaO_4$ $(M+Na)^+$ calcd 279.0628, obsd 279.0620.

4.1.2.4. (*E*)-3-(4-Hydroxy-3-methoxyphenyl)-2-phenylacrylic acid (1d). Yellow solid, 97% yield. ^{1}H NMR (500 MHz, DMSO-d_6) δ 9.47 (s, 1 H, OH), 7.64 (s, 1 H, vinylic H), 7.40 (t, 2 H, *J* = 7.5 Hz, 3-H, 5-H), 7.33 (t, 1 H, *J* = 7.5 Hz, 4-H), 7.17 (d, 2 H, *J* = 8.0 Hz, 2-H, 6-H), 6.66 (dd, 1 H, *J* = 8.0, 2.0 Hz, 6′-H), 6.61 (d, 1 H, *J* = 8.0 Hz, 5′-H), 6.40 (d, 1 H, *J* = 2.0 Hz, 2′-H), 3.69 (s, 3 H, OCH_3); ^{13}C NMR (100 MHz, DMSO-d_6) δ 169.2, 148.7, 147.5, 140.2, 137.8, 130.3, 129.3, 128.0, 126.2, 126.0, 115.8, 113.7, 55.3; LRMS (ESI-) *m/z* 269 $(M\text{-}H)^-$.

4.1.2.5. (*E*)-3-(3-Ethoxy-4-hydroxyphenyl)-2-phenylacrylic acid (1e). Yellow solid, 88% yield. ^{1}H NMR (500 MHz, $CDCl_3$ + 1 drop of CD_3OD) δ 7.75 (s, 1 H, vinylic H), 7.37 (t, 2 H, *J* = 7.5 Hz, 3-H, 5-H), 7.30 (t, 1 H, *J* = 7.5 Hz, 4-H), 7.22 (d, 2 H, *J* = 7.5 Hz, 2-H, 6-H), 6.74 (dd, 1 H, *J* = 8.0, 1.5 Hz, 6′-H), 6.70 (d, 1 H, *J* = 8.0 Hz, 5′-H), 6.32 (d, 1 H, *J* = 1.5 Hz, 2′-H), 3.52 (q, 2 H, *J* = 7.5 Hz, CH_2CH_3), 1.17 (t, 3 H, *J* = 7.5 Hz, CH_2CH_3); ^{13}C NMR (100 MHz, $CDCl_3$ + 1 drop of CD_3OD) δ 170.6, 147.4, 145.5, 141.5, 136.9, 130.0, 129.5, 129.0, 127.7, 126.6, 126.4, 114.4, 113.2, 63.9, 14.7; LRMS (ESI-) *m/z* 283 $(M\text{-}H)^-$.

4.1.2.6. (*E*)-3-(3-Hydroxy-4-methoxyphenyl)-2-phenylacrylic acid (1f). Yellowish white solid, 99% yield. ^{1}H NMR (500 MHz, DMSO-d_6) δ 8.87 (s, 1 H, OH), 7.59 (s, 1 H, vinylic H), 7.37 (t, 2 H, *J* = 7.5 Hz, 3-H, 5-H), 7.33 (t, 1 H, *J* = 7.5 Hz, 4-H), 7.13 (d, 2 H, *J* = 7.5 Hz, 2-H, 6-H), 6.72 (d, 1 H, *J* = 8.5 Hz, 5′-H), 6.50 (dd, 1 H, *J* = 8.5, 2.0 Hz, 6′-H), 6.42 (d, 1 H, *J* = 2.0 Hz, 2′-H), 3.69 (s, 3 H, OCH_3); ^{13}C NMR (100 MHz, DMSO-d_6) δ 169.2, 149.4, 146.5, 139.9, 137.4, 131.1,

130.1, 129.2, 128.1, 127.7, 123.4, 117.9, 112.1, 56.1; LRMS (ESI-) *m/z* 269 $(M-H)^-$.

4.1.2.7. (*E*)-3-(4-Hydroxy-3-methylphenyl)-2-phenylacrylic acid (1g). Yellowish white solid, 99% yield. ^{1}H NMR (500 MHz, $CDCl_3$ + 1 drop of CD_3OD) δ 7.72 (s, 1 H, vinylic H), 7.31 (t, 2 H, J = 7.5 Hz, 3-H, 5-H), 7.29 (t, 1 H, J = 7.5 Hz, 4-H), 7.16 (d, 2 H, J = 7.5 Hz, 2-H, 6-H), 6.73 (d, 1 H, J = 2.0 Hz, 2′-H), 6.64 (dd, 1 H, J = 8.5, 2.0 Hz, 6′-H), 6.45 (d, 1 H, J = 8.5 Hz, 5′-H), 1.96 (s, 3 H, CH_3); ^{13}C NMR (100 MHz, $CDCl_3$ + 1 drop of CD_3OD) δ 170.8, 156.5, 141.6, 136.9, 134.3, 130.1, 129.9, 129.0, 128.8, 127.6, 126.2, 124.5, 114.6, 15.9; LRMS (ESI-) *m/z* 253 $(M-H)^-$.

4.1.2.8. (*E*)-3-(2-Hydroxyphenyl)-2-phenylacrylic acid (1h). White solid, 89% yield. ^{1}H NMR (400 MHz, $CDCl_3$ + 1 drop of CD_3OD) δ 8.15 (s, 1 H, vinylic H), 7.27 – 7.22 (m, 3 H, 3-H, 4-H, 5-H), 7.18 (d, 2 H, J = 7.6 Hz, 2-H, 6-H,), 6.98 (t, 1 H, J = 8.0 Hz, 5′-H), 6.71 (d, 1 H, J = 8.0 Hz, 6′-H), 6.55 (d, 1 H, J = 8.0 Hz, 2′-H), 6.41 (t, 1 H, J = 8.0 Hz, 3′-H); ^{13}C NMR (100 MHz, $CDCl_3$ + 1 drop of CD_3OD) δ 170.7, 156.3, 136.4, 136.2, 131.8, 130.6, 130.5, 130.2, 128.5, 127.8, 122.1, 119.4, 115.8; LRMS (ESI-) *m/z* 239 $(M-H)^-$.

4.1.2.9. (*E*)-3-(3-Hydroxyphenyl)-2-phenylacrylic acid (1i). Off-white solid, 99% yield. ^{1}H NMR (500 MHz, $CDCl_3$ + 1 drop of CD_3OD) δ 7.78 (s, 1 H, vinylic H), 7.34 (t, 2 H, J = 7.5 Hz, 3-H, 5-H), 7.31 (t, 1 H, J = 7.5 Hz, 4-H), 7.21 (d, 2 H, J = 7.5 Hz, 2-H, 6-H), 6.97 (t, 1 H, J = 8.0 Hz, 5′-H), 6.66 (d, 1 H, J = 8.0 Hz, 6′-H), 6.54 (d, 1 H, J = 8.0 Hz, 4′-H), 6.47 (s, 1 H, 2′-H); ^{13}C NMR (100 MHz $CDCl_3$ + 1 drop of CD_3OD) δ 170.6, 156.4, 141.3, 136.3, 136.0, 132.4, 130.0, 129.4, 128.7, 127.8, 122.8, 117.3, 116.7; LRMS (ESI-) *m/z* 239 $(M-H)^-$.

4.1.2.10. (*E*)-3-(4-Hydroxy-3,5-dimethoxyphenyl)-2-phenylacrylic acid (1j). Yellowish grey solid, 96% yield. ^{1}H NMR (500 MHz, $CDCl_3$ + 1 drop of CD_3OD) δ 7.75 (s, 1 H, vinylic H), 7.39 (t, 2 H, J = 7.5 Hz, 3-H. 5-H), 7.30 (t, 1 H, J = 7.5 Hz, 4-H), 7.24 (d, 2 H, J = 7.5 Hz, 2-H, 6-H),

6.29 (s, 2 H, 2′-H, 6′-H), 3.53 (s, 6 H, 2□OCH_3); ^{13}C NMR (100 MHz, $CDCl_3$ + 1 drop of CD_3OD) δ 174.8, 146.8, 141.6, 136.8, 136.4, 130.1, 129.0, 127.9, 125.7, 108.3, 56.0; LRMS (ESI-) *m/z* 299 $(M-H)^-$.

4.1.2.11. (*E*)-3-(3-Bromo-4-hydroxyphenyl)-2-phenylacrylic acid (1k). Yellowish white solid, 96% yield. ^{1}H NMR (500 MHz, $CDCl_3$ + 1 drop of CD_3OD) δ 7.69 (s, 1 H, vinylic H), 7.35 (t, 2 H, J = 7.5 Hz, 3-H, 5-H), 7.32 (t, 1 H, J = 7.5 Hz, 4-H), 7.17 (d, 2 H, J = 7.5 Hz, 2-H, 6-H), 7.11 (d, 1 H, J = 2.0 Hz, 2′-H), 6.78 (dd, 1 H, J = 8.5, 2.0 Hz, 6′-H), 6.63 (d, 1 H, J = 8.5 Hz, 5′-H); ^{13}C NMR (100 MHz, $CDCl_3$ + 1 drop of CD_3OD) δ 170.3, 154.4, 139.6, 136.1, 135.5, 131.4, 131.1, 129.8, 128.9, 128.1, 128.0, 115.9, 109.9; LRMS (ESI-) *m/z* 317 $(M-H)^-$, 319 $(M+2-H)^-$.

4.1.2.12. (*E*)-3-(3,5-Dibromo-4-hydroxyphenyl)-2-phenylacrylic acid (1l). Yellow solid, 95% yield. ^{1}H NMR (500 MHz, DMSO-d_6) δ 12.66 (brs, 1 H, COOH), 10.29 (brs, 1 H, OH), 7.61 (s, 1 H, vinylic H), 7.42 – 7.37 (m, 3 H, 3-H, 4-H, 5-H), 7.17 – 7.13 (m, 4 H, 2-H, 6-H, 2′-H, 6′-H); ^{13}C NMR (100 MHz, DMSO-d_6) δ 168.7, 151.9, 136.9, 136.6, 134.8, 133.6, 129.9, 129.4, 129.4, 128.5, 112.0; LRMS (ESI-) *m/z* 395 $(M-H)^-$, 397 $(M+2-H)^-$, 399 $(M+4-H)^-$.

4.1.2.13. (*Z*)-3-(3,5-dibromo-4-hydroxyphenyl)-2-phenylacrylic acid (1l′). Yellowish white solid, 97% yield. ^{1}H NMR (500 MHz, $CDCl_3$ + 1 drop of CD_3OD) δ 7.54 (s, 2 H, 2′-H, 6′-H), 7.41 (d, 2 H, J = 7.5 Hz, 2-H, 6-H), 7.31 (t, 1 H, J = 7.5 Hz, 3-H, 5-H), 7.27 (t, 1 H, J = 7.5 Hz, 4-H), 7.26 (t, 1 H, J = 7.5 Hz, 5-H), 6.70 (s, 1 H, vinylic H); ^{13}C NMR (100 MHz, $CDCl_3$ + 1 drop of CD_3OD) δ 171.4, 150.3, 136.7 136.1, 134.4, 132.1, 128.7, 128.5, 127.1, 126.5, 110.7; LRMS (ESI-) *m/z* 395 $(M-H)^-$, 397 $(M+2-H)^-$, 399 $(M+4-H)^-$.

4.2. Docking study of 2,3-DPA derivative 1c and kojic acid

The docking study procedure used was performed as previously described.[34] Chem3D Pro 12.0

software was used to create a 3D structure for **1c**. AutoDock Vina and chimera software were used to calculate binding scores between **1c** or kojic acid and tyrosinase. The three-dimensional structure of tyrosinase (PDB ID: 2Y9X, *Agaricus Bisporus*) was obtained from the Protein Data Bank, and LigandScout software ver. 4.3.0 was used to generate a pharmacophore model showing possible interactions between **1c** and amino acid residues of tyrosinase.

4.3. Biological Investigation

4.3.1. Mushroom tyrosinase inhibition assay of the fifteen 2,3-DPA derivatives

Mushroom tyrosinase inhibition was assayed as previously described.[35] Ten μL of 2,3-DPA derivatives (**1a** – **1n** and **1l′**, 25 μM) and 20 μL of tyrosinase solution (1000 units per mL) were added to 170 μL solution of substrate solution (14.7 mM of phosphate buffer and 293 μL of L-tyrosine solution, 1:1, v/v), mixed, and added to 96-well plates, which were then incubated for 30 minutes at 37^0C. Tyrosinase inhibition percentages were calculated from optical densities measured at 450 nm using a VersaMax shaking microplate reader. Kojic acid (25 μM) was used as the control. Three independent experiments were performed. The formula used to calculate % inhibition was;

%Inhibition = [1-(A/B) x 100]

where A is the absorbance of a 2,3-DPA derivative and B is the absorbance of the non-treated control.

4.3.2. Cell culture

B16F10 cells (a murine melanoma cell-line) were obtained from the American Type Culture

Collection (ATCC, VS, USA). Cells were cultured in DMEM (Dulbecco's medium) containing 10% fetal bovine serum (FBS), 100 µg/mL streptomycin, and 100 IU/ml penicillin in a humidified 5% CO_2 atmosphere at 37^0C. These cells were subsequently used for cell viability, tyrosinase inhibition, and melanin content assays.

4.3.3. Determination of the cell viabilities of B16F10 melanoma cells treated with compound 1c

A previously described WST-8 assay was used to assess cell viabilities.[36] Cells were incubated in a 96-well plate at $5x10^4$ cells per well in a humidified 5% CO_2 atmosphere for 24 h at 37^0C. Compound **1c** was added to the cells at concentrations of 0, 5, 10, or 25 µM and cells were re-incubated for 24 h under the same conditions. Cells were then treated with WST-8 reagents and incubated for 1 h at 37^0C. The cell viabilities were determined using the EZ-Cytox assay (EZ-3000, Daeil Lab Service, Seoul) by reading optical densities at 450 nm. Experiments were repeated three times.

4.3.4. Tyrosinase inhibition assay in B16F10 melanoma cells

The tyrosinase inhibition assay was performed as previously described with slight changes.[37] Briefly, B16F10 cells were inoculated at $5x10^4$ cells per well into 96-well plates and incubated in a humidified 5% CO_2 atmosphere for 24 h at 37^0C. Cells were then treated with α-MSH (1 µM) and kojic acid (25 µM) or compound **1c** (0, 5, 10, or 25 µM) and re-incubated for 24 h under the same conditions. Cells were then washed with PBS buffer, lysed with lysis buffer (100 µL containing 50 mM PBS, 0.1 mM PMSF (5 µL), and Triton X-100 (5 µL)), and frozen at -80 ^{0}C for 30 min. Cell lysates were then centrifuged at 12,000 rpm for 30 min at 4 ^{0}C, transferred to 96-well plates in a total volume of 100 µL (80 µL of lysate supernatant and 20 µL of 10 mM L-dopa), and incubated for 30 min at 37^0C. Tyrosinase inhibition was quantified by measuring optical densities

at 500 nm using a Tecan, Mannedorf microplate reader. The experiment was performed in triplicate.

4.3.5. Anti-melanogenic assays performed using B16F10 cells

The anti-melanogenic effect of compound **1c** was determined as previously described melanin assay with minor changes.[38] In brief, B16F10 cells were inoculated at $5x10^4$ cells per well in 96-well plates and incubated in a humidified 5% CO_2 atmosphere for 24 h at 37^0C. Cells were then treated with α-MSH (1 µM) and kojic acid (25 µM) or compound **1c** (0, 5, 10, or 25 µM) and re-cultured for 24 h under the same conditions. Cells were then cleaned with PBS buffer and melanin contents were dissolved by incubating cells with 1 N NaOH solution (200 µL) at 50 ^{0}C for 1 h. Melanin contents were determined by measuring optical densities at 405 nm in 96-well plates using a Tecan, Mannedorf microplate reader. The experiment was performed in triplicate.

4.3.6. Procedure for anti-oxidant activity determination

A slightly modified version of a previously described DPPH radical scavenging assay was used to assess anti-oxidant activities.[39] Briefly, 20 µL of a solution (in DMSO) of each 2,3-DPA derivative was mixed with 180 µL of DPPH methanol solution (0.2 mM) in 96-well plates. L-Ascorbic acid was used as the positive control. Mixture were then incubated for 30 min in the dark, and antioxidant activities were determined by measuring absorbances at 517 nm using a VersaMax microplate reader. Experiments were performed in triplicate. The formula used to determine DPPH radical scavenging activity was;

Radical scavenging activity (%) = [(Ac-As) x 100/Ac]

where Ac is absorbance of the non-treated control and As is the absorbance of a sample containing

a 2,3-DPA derivative.

4.3.6. Statistical analysis

Statistical analysis was determined using GraphPad Prism 5 software (La Jolla, CA, USA). All experiments were performed in triplicate, and results are expressed as means ± SEMs. The significances of intergroup differences were determined by one-way ANOVA and Tukey's test. *P*-values < 0.05 were considered to be statistically significant.

Acknowledgment

This research was supported by the Basic Science Research Program through the National Research Foundation of Korea (NRF) funded by the Ministry of Education (NRF-2017R1D1A1B03027888).

References

1. Pillaiyar T, Namasivayam V, Manickam M, Jung SH. Inhibitors of Melanogenesis: An Updated Review. *Journal of medicinal chemistry.* 2018.
2. Brenner M, Hearing VJ. The protective role of melanin against UV damage in human skin. *Photochemistry and photobiology.* 2008;84(3): 539-549.
3. Bonaventure J, Domingues MJ, Larue L. Cellular and molecular mechanisms controlling the migration of melanocytes and melanoma cells. *Pigment cell & melanoma research.* 2013;26(3): 316-325.
4. Borovansky J, Riley PA. *Melanins and Melanosomes: Biosynthesis, Structure, Physiological and Pathological Functions*: John Wiley & Sons; 2011.
5. Costin G-E, Hearing VJ. Human skin pigmentation: melanocytes modulate skin color in response to stress. *The FASEB journal.* 2007;21(4): 976-994.
6. Coudrier E. Myosins in melanocytes: to move or not to move? *Pigment cell research.* 2007;20(3): 153-160.
7. Wu X, HAMMER III JA. Making sense of melanosome dynamics in mouse melanocytes. *Pigment cell research.* 2000;13(4): 241-247.
8. Ahn SJ, Koketsu M, Ishihara H, et al. Regulation of melanin synthesis by selenium-containing carbohydrates. *Chemical and pharmaceutical bulletin.* 2006;54(3): 281-286.
9. Iozumi K, Hoganson GE, Pennella R, Everett MA, Fuller BB. Role of tyrosinase as the determinant of pigmentation in cultured human melanocytes. *Journal of Investigative Dermatology.* 1993;100(6): 806-811.
10. Li G, Ju HK, Chang HW, Jahng Y, Lee S-H, Son J-K. Melanin biosynthesis inhibitors from the bark of Machilus thunbergii. *Biological and Pharmaceutical Bulletin.* 2003;26(7): 1039-1041.

11. Ünver N, Freyschmidt□Paul P, Hörster S, et al. Alterations in the epidermal–dermal melanin axis and factor XIIIa melanophages in senile lentigo and ageing skin. *British Journal of Dermatology.* 2006;155(1): 119-128.

12. Cavalieri EL, Li K-M, Balu N, et al. Catechol ortho-quinones: the electrophilic compounds that form depurinating DNA adducts and could initiate cancer and other diseases. *Carcinogenesis.* 2002;23(6): 1071-1077.

13. Hasegawa T. Tyrosinase-expressing neuronal cell line as in vitro model of Parkinson's disease. *International journal of molecular sciences.* 2010;11(3): 1082-1089.

14. Tessari I, Bisaglia M, Valle F, et al. The reaction of α-synuclein with tyrosinase: Possible implications for parkinson disease. *Journal of Biological Chemistry.* 2008.

15. Vontzalidou A, Zoidis G, Chaita E, et al. Design, synthesis and molecular simulation studies of dihydrostilbene derivatives as potent tyrosinase inhibitors. *Bioorganic & medicinal chemistry letters.* 2012;22(17): 5523-5526.

16. Greggio E, Bergantino E, Carter D, et al. Tyrosinase exacerbates dopamine toxicity but is not genetically associated with Parkinson's disease. *Journal of neurochemistry.* 2005;93(1): 246-256.

17. Ullah S, Son S, Yun HY, Kim DH, Chun P, Moon HR. Tyrosinase inhibitors: a patent review (2011-2015). *Expert Opinion on Therapeutic Patents.* 2016;26(3): 347-362.

18. A. Hassan, A. Reem, B. Rodney,. *Screening methods for identifying ligands that target HCV-E2 binding sites on CD81 and therapeutic uses thereof for treating viral infections and associated diseases*, 2014, WO 2014081856 A2.

19. Kumar S, Sapra S, Kumar R, et al. Synthesis of combretastatin analogs: evaluation of in vitro anticancer activity and molecular docking studies. *Medicinal Chemistry Research.* 2012;21(11): 3720-3729.

20. L. Jing, H. Guangjie, Y. Xinyi, W. Shuli, C. Liying, H. Xiaoyun, S. Liang., *Vascular endothelial growth factor inhibitor aerosol pharmaceutical composition*, 2017, CN 106890163 A.

21. M. Adnan M.M.; C. Xiaodon, M. Edmund J., *Protein tyrosine phosphatase-inhibiting compounds*, 2002, US6388076B1.

22. B. Tanja, Hecker, Anaies,. *Functionalized calcium carbonate for sun protection boosting*, 2018, EP 3360601 A1.

23. C. Glenn,. *Dry powder inhaler compositions*, 2014, US 20140116434 A.

24. Son S, Kim H, Yun HY, et al. (E)-2-Cyano-3-(substituted phenyl) acrylamide analogs as potent inhibitors of tyrosinase: A linear β-phenyl-α, β-unsaturated carbonyl scaffold. *Biorg Med Chem.* 2015;23(24): 7728-7734.

25. Yun HY, Do Hyun Kim SS, Ullah S, et al. Design, synthesis, and anti-melanogenic effects of (E)-2-benzoyl-3-(substituted phenyl) acrylonitriles. *Drug design, development and therapy.* 2015;9: 4259.

26. Kim SJ, Yang J, Lee S, et al. The tyrosinase inhibitory effects of isoxazolone derivatives with a (Z)-β-phenyl-α, β-unsaturated carbonyl scaffold. *Biorg Med Chem.* 2018.

27. Do Hyun Kim SJK, Ullah S, Yun HY, Chun P, Moon HR. Design, synthesis, and antimelanogenic effects of (2-substituted phenyl-1, 3-dithiolan-4-yl) methanol derivatives. *Drug Des Devel Ther.* 2017;11: 827.

28. Lee EK, Kim JH, Moon KM, et al. Tyrosinase Inhibitory Effect of (E)-2-(substituted benzylidene)-2, 3-dihydro-1H-cyclopenta [a] naphthalen-1-one Derivatives. *Journal of*

Life Science. 2017;27(2): 139-148.

29. Jung HJ, Lee MJ, Park YJ, et al. A novel synthetic compound,(Z)-5-(3-hydroxy-4-methoxybenzylidene)-2-iminothiazolidin-4-one (MHY773) inhibits mushroom tyrosinase. *Biosci Biotechnol Biochem.* 2018;82(5): 759-767.

30. Gaukroger K, Hadfield JA, Hepworth LA, Lawrence NJ, McGown AT. Novel Syntheses of Cis and Trans Isomers of Combretastatin A-4. *The Journal of Organic Chemistry.* 2001;66(24): 8135-8138.

31. Johnson JR. The P erkin Reaction and Related Reactions. *Organic reactions.* 2004;1: 210-265.

32. Ha YM, Kim J-A, Park YJ, et al. Synthesis and biological activity of hydroxybenzylidenyl pyrrolidine-2, 5-dione derivatives as new potent inhibitors of tyrosinase. *MedChemComm.* 2011;2(6): 542-549.

33. Kim C, Noh S, Park Y, et al. A Potent Tyrosinase Inhibitor,(E)-3-(2, 4-Dihydroxyphenyl)-1-(thiophen-2-yl) prop-2-en-1-one, with Anti-Melanogenesis Properties in α-MSH and IBMX-Induced B16F10 Melanoma Cells. *Molecules.* 2018;23(10): 2725.

34. Bagherzadeh K, Shirgahi Talari F, Sharifi A, Ganjali MR, Saboury AA, Amanlou M. A new insight into mushroom tyrosinase inhibitors: docking, pharmacophore-based virtual screening, and molecular modeling studies. *Journal of Biomolecular Structure and Dynamics.* 2015;33(3): 487-501.

35. Hyun SK, Lee W-H, Jeong DM, Kim Y, Choi JS. Inhibitory effects of kurarinol, kuraridinol, and trifolirhizin from Sophora flavescens on tyrosinase and melanin synthesis. *Biological and Pharmaceutical Bulletin.* 2008;31(1): 154-158.

36. Ishiyama M, Tominaga H, Shiga M, Sasamoto K, Ohkura Y, Ueno K. A combined assay of cell vability and in vitro cytotoxicity with a highly water-soluble tetrazolium salt, neutral red and crystal violet. *Biol Pharm Bull.* 1996;19(11): 1518-1520.

37. Bae SJ, Ha YM, Kim J-A, et al. A novel synthesized tyrosinase inhibitor:(E)-2-((2, 4-dihydroxyphenyl) diazenyl) phenyl 4-methylbenzenesulfonate as an azo-resveratrol analog. *Bioscience, biotechnology, and biochemistry.* 2013;77(1): 65-72.

38. Chen L-G, Chang W-L, Lee C-J, Lee L-T, Shih C-M, Wang C-C. Melanogenesis inhibition by gallotannins from Chinese galls in B16 mouse melanoma cells. *Biological and Pharmaceutical Bulletin.* 2009;32(8): 1447-1452.

39. Matos M, Varela C, Vilar S, et al. Design and discovery of tyrosinase inhibitors based on a coumarin scaffold. *RSC Advances.* 2015;5(114): 94227-94235.

Highlights

- Fifteen 2,3-DPA derivatives were designed and synthesized via Perkin reaction
- (*Z*)-2,3-DPA derivative (**1l'**) was reported for the first time as a major product
- Mushroom tyrosinase and B16F10 cells were used for *in vitro* studies
- **1c** significantly decreased the activity of mushroom and cellular tyrosinase
- In docking studies, **1c** strongly bind to tyrosinase than kojic acid

Graphical abstract

Antioxidant, anti-tyrosinase and anti-melanogenic effects of (*E*)-2,3-diphenylacrylic acid derivatives

Sultan Ullah[a,§], Yujin Park[a,§], Chaeun Park[a], Sanggwon Lee[a], Dongwan Kang[a], Jungho Yang[a], Jinia Akter[a], Pusoon Chun[b], Hyung Ryong Moon[a,*]